

PAPER III

**Limitations of current
formulations when decreasing the
coating layer thickness of papers
for inkjet printing**

In: Industrial and Engineering Chemistry Research
2011(50)12, pp. 7251–7263.

Copyright 2011 American Chemical Society.

Reprinted with permission from American
Chemical Society.

Limitations of Current Formulations when Decreasing the Coating Layer Thickness of Papers for Inkjet Printing

Taina Lamminmäki,^{*,†} John Kettle,[†] Hille Rautkoski,[†] Annaleena Kokko,[†] and Patrick Gane^{‡,§}

[†]VTT Technical Research Centre of Finland, Biologinkuja 7, FI-02150 Espoo, Finland

[‡]Department of Forest Products Technology, School of Chemical Technology, Aalto University, P.O. Box 16300, FI-00076 Aalto, Finland

[§]Omya Development AG, CH-4665 Oftringen, Switzerland.

ABSTRACT: The porous network structure of a coating layer has a major effect on how quickly inkjet ink penetrates into the coated paper, and how large the pore volume is determines the capacity for ink volume uptake within the coating layer. If the penetration rate and/or pore volume are insufficient, the ink colors stay too long on the surface, resulting in undesirable mixing (intercolor bleeding) and trans-surface wicking (feathering). The aim of this work was to clarify whether it is possible to decrease the coating layer thickness of the specialty inkjet layer and still produce an inkjet printed surface using dye-based inks with low bleeding and, thereby, to define the reasons for limitations with respect to coat weight reduction. The online study of printed figures following printing nozzles on a high-speed inkjet printing press, by means of optical image capture, showed that the tendency for intercolor bleeding depends strongly on the coating layer thickness. As the printing speed increases, the pore network structure of the coating layer becomes increasingly important. The results show that, under the external pressure, caused by the surface tension and impact of the ink droplets themselves, the permeability of the coating layer dominates after at least 4 ms from the time of ink application. The coating pigment selection and the amount of poly(vinyl alcohol) binder did not influence this permeability onset time. Permeability allows the required ink volumes eventually to be absorbed, even if the total porosity of the coating is insufficient at low coat weight.

1. BACKGROUND

A good-quality dye-based inkjet ink-printable paper currently means that the base paper is coated with special pigments and special binders.^{1–3} A great deal of interest is focused on developing cheaper inkjet coatings with similar inkjet printability properties shown by the specialty coated papers available today. One way to reduce the costs of paper is to decrease the coat weight.

The pore size distribution and network structure of the coating layer, together with the type of binder present, determine how quickly ink penetrates into the available pore volume. It is the pore volume of the uppermost coating layer that provides the region where the inkjet ink can be held during the ink setting process.^{4–6} The use of smaller-diameter pigment pores in the coating structure provides a coating layer that directs penetration of the inkjet ink droplets mainly in the z direction of the structure, rather than allowing them to spread along the structure⁷ surface, and the inclusion of fine pores increases capillarity and, therefore, the sorption rate. This is one way to diminish the tendency for bleeding on coated paper. The speed of liquid absorption into the coating pore structure and the total amount of liquid penetrated have been studied in detail.^{2,4,8–11} Several studies have also been reported in the literature on the potential for inkjet ink droplet penetration into coating layer structures that contain different coating pigments, binders, and additives as detected by means of the contact angle of a sessile or dynamic drop^{2,7,12–14} or its volume change with time. In these studies, the ink penetration rate inside the coated paper structure was not clarified. More recently, the role of the surface morphology (roughness) of the underlying polymer layers present in the

highest-quality inkjet printing products has been studied in other applications, such as the printing of electronics.^{15,16} The more basic phenomenon of low-viscosity liquid sorption in a capillary tube has also been studied,^{17,18} but the diameters of capillaries in these studies were in the range of micrometers rather than nanometers.

Ridgway et al.⁴ summarized the existing theoretical knowledge surrounding the sorption phenomena of coating layer structures by applying the Lucas–Washburn, Bosanquet, Szekeley, and Sorbie equations and showing their relative merits and shortcomings when considering the short time scales involved during initial pore filling. The liquid front velocity upon first contact depends inversely on the radius of the capillaries. Later in the absorption process, the connectivity and pore size ratio dominate. The important controlling component in the liquid movement in an empty pore is the capillary element aspect ratio, that is, the length of the capillary divided by its radius, l/r . There seems to be an optimal aspect ratio for fastest filling, and it falls in the range $0.1 < l/r < 10$ for pores with $l < 100 \mu\text{m}$. The limited aspect ratio range is due to the viscosity-independent initial stage of wetting predicted by Bosanquet and Szekeley, occurring over ~ 10 ns, which favors entry into nanopores that are of similar dimensions in both radius and length. This knowledge related to the throatlike structures of capillaries provides a better

Received: October 18, 2010

Accepted: May 9, 2011

Revised: May 9, 2011

Published: May 09, 2011

opportunity to simulate the liquid penetration process at the shortest time scales.

The penetration speed at different depths of the substrate structure, including the ability to transmit liquid into the underlying precoat or base paper, has not been studied as widely. In the area of offset coatings, the role of coat weight has been studied more. Xiang and Bousfield¹⁹ showed, for example, that different drying conditions produced different pore structures in the coating layer. A low coat weight of clay/ground calcium carbonate blends (80/20 pph) produces more porous structures than a high coat weight. In a Micro-Tack tester analyzer, a low-coat-weight coating displayed a more rapid offset ink tack rise and earlier ink tack decay than the corresponding high-coat-weight coating. These effects are related to coating consolidation and shrinkage.

In contrast to the shortest-time-scale nonequilibrium capillary-induced absorption discussed above, equilibrium liquid uptake under external pressure and viscous laminar flow can be derived from the Navier–Stokes equation as the Poiseuille equation (eq 1), showing the connection between the penetration rate per unit cross-sectional area [$dV(t)/dt$] and the equivalent permeation radius, r_{perma} , representing the unit area in question

$$\frac{dV_{\alpha}(t)}{dt} = \pi \frac{(r_{\text{perma}})^4 \Delta P}{8\eta \Delta L} \quad (1)$$

where $V_{\alpha}(t)$ is the volume of flow across a unit area of the sample (m^3), t is the time (s), r_{perma} is the permeation radius for a unit area of the sample (m), ΔP is the pressure drop (N m^{-2}), ΔL is the sample depth (m), and η is the fluid viscosity (N s m^{-2}).

Darcy's law (eq 2) is also a special solution of the Navier–Stokes equation and follows the condition of Poiseuille flow through the sample, such that there is a flux of liquid [$dV(t)/dt$] forced through a saturated porous medium under the action of a pressure gradient⁸

$$\frac{dV(t)}{dt} = -\frac{K \Delta P}{\eta \Delta L} A \quad (2)$$

The term K is the permeability of the porous medium. In the case of inkjet ink setting, K describes the flow when the wetting front lies deep within the coating structure or when the inertia of the impacting droplet causes initial penetration into the top layer of the coating. Darcy's law assumes that the pores fill completely with the liquid, that is, that permeation operates under conditions of saturation.

Alternative expressions have been established for penetration rate,¹⁷ but the initial absorption into the fine pores was not taken into account in that study. More recently, Ridgway et al.⁴ based comparisons on either inertial retardation or energy terms related to pore entry loss and adopted the interpretation of plug flow occurring in nanopores prior to the establishment of the viscous drag of liquid, together with inertial retardation prior to entry into large pores, following the Bosanquet expression.

The role of coating layer thickness on the inkjet-printed surface bleeding was studied by Nilsson and Fogden³ and Glittenberg et al.²⁰ Their results showed that the coating pigment size has an effect on the inkjet-printed color range and print density. Larger pigment particles provided a lower print density, and with the larger pigment size, a higher coat weight gave a lower color range. Styrene–butadiene latex-containing coatings

Table 1. Coating Colors on the Plastic Film

component	color 1	color 2	color 3	color 4
PCC (specialty inkjet pigment)	100	100		
GCC (offset coating pigment)			100	100
PVOH	7	15	7	15

were shown to behave differently than coatings containing poly(vinyl alcohol) or carboxymethyl cellulose.

The aim of this work was to clarify how inkjet ink penetrates through the different thicknesses of a coating layer and, thus, to the underlying precoat or base paper. The focus here is on the role of diffusion in soluble binders, which adds time-scale and pore-structure information to the original findings. Topcoatings were applied to wood-free fine paper using a curtain coater. The impact of coat weight on the inkjet ink imbibition was studied as a function of soluble poly(vinyl alcohol) (PVOH) binder. In addition to the commonly used measurements of paper properties, a capacitance-based liquid absorption device, Clara,²¹ was used to determine ink permeation, and online imaging was used to monitor the bleeding tendency of two inkjet inks applied with a Versamark VX5000e high-speed inkjet press.

2. MATERIALS

2.1. Coating Colors on Plastic Film. Inkjet ink penetration into coating layers alone, having different thickness, was first studied by applying the coating color to impermeable plastic film. Table 1 introduces the studied coating color formulations. The high-porosity inkjet coatings contained a specialty precipitated calcium carbonate (PCC, JetCoat 30) from Minerals Technology Europe. The weight-median pigment particle diameter (NanoSight) was 20–30 nm, with a size distribution showing some larger particles in the range of 250 nm. The specific surface area [Brunauer–Emmett–Teller (BET), ISO 9277] was $73.9 \text{ m}^2 \text{ g}^{-1}$, and the pigment had a primarily calcitic rhombohedral structure. The low-porosity coating constituted a typical offset-coating pigment consisting of ground calcium carbonate (GCC, Hydrocarb 90) provided by Omya AG. The weight-median pigment particle size was $0.65 \mu\text{m}$, and the specific surface area was $10.7 \text{ m}^2 \text{ g}^{-1}$. The binder was poly(vinyl alcohol) (PVOH, Mowiol 40-88 provided by Clariant International AG), which had a degree of hydrolysis of $(87.7 \pm 1.0)\%$. The colors were applied with an Erichsen draw-down coater using a speed of 1.4 m min^{-1} and spiral applicators (Spiral Film Applicator, model 358). The coatings were dried for 5 min inside an oven at $105 \text{ }^\circ\text{C}$.

2.2. Coating Composition in Curtain-Coating Trials. The role of coating layer thickness on the fine paper surface was studied with coatings containing the specialty PCC pigment (JetCoat 30). The coating colors had 7 or 15 pph of poly(vinyl alcohol) (Mowiol 40-88) based on 100 pph of pigment. All colors had 0.2 pph surfactant, Lumiten DF provided by BASF. Lumiten DF is the sodium salt of an ester of sulfosuccinic acid and an isotridecanol ethoxylate. The inclusion of surfactant acted to stabilize the curtain formation.

The coatings were applied to a precoated fine paper provided by Stora Enso having a grammage of 78 gm^{-2} . By using the precoated paper, we wanted to prevent the topcoating penetration into the base paper structure. The findings, therefore, are not directly transferable to rough nonprecoated substrates, in which the fiber-mat base paper frequently provides the absorption sink

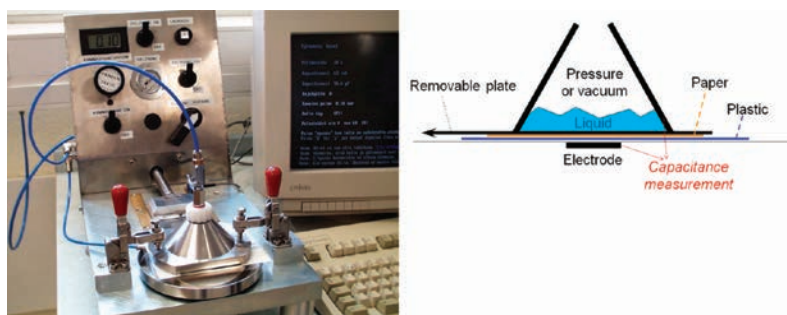


Figure 1. Clara device and its working principle.

in the case of lighter-weight inkjet coatings. However, the use of a typical low-cost precoat might be more effective with respect to cost/performance tradeoffs than the loss of specialty coating into the surface voids. Furthermore, the precoat layer can act as an absorption sink, preventing the wetting, and thus cockling, of the fiber base paper.

The coating trial was performed on a Metso pilot coater using a curtain slide applicator. The coating speed was varied from 1000 to 600 m min^{-1} depending on the weight of the applied coating. The highest speed was used when the coat weight was the lowest and vice versa. The final moisture content of the coated web was 5.1–5.4 wt %. This means that the drying temperature had to be increased when the coat weight was high. It was not possible to achieve a coat weight of 10 gm^{-2} with the 7 pph PVOH-containing coating because of the low solids content of the color. The coated papers were printed with a Versamark VX5000e high-speed inkjet press, which had aqueous-based dye inks.

3. TESTING METHODS

The thickness of samples was measured according to standard ISO 12625-3:05. The air permeance of coated papers was measured using a Parker-Print Surf testing machine (20 kPa) following the ISO 5636/1 standard. The porosity of coating layers was measured independently by silicon-oil absorption at 1 bar pressure and by mercury porosimetry. In the Si-oil measurement, the porosity was calculated from the weights of dry and Si-oil-immersed samples. The results reported are the averages of three measurements each. A Micrometrics AutoPore IV mercury porosimeter was used, including the Pore-Comp correction to account for penetrometer expansion, mercury compression, and compression of the sample skeletal material, expressed in terms of cumulative pore volume, according to the method Gane et al.²² The contact angles of water on the surfaces were measured with Fibro 1100 DAT instrument with a 2 μL drop, as the apparent contact angle after 0.1 s.

The absorption time of ink was measured with a DIGAT device (Dynamic Ink Gloss and Absorption Tester).¹¹ It measures the absorption time by detecting changes in the gloss level as the surface liquid retreats into the pore structure and the remaining ink components dry. The measurement started from the moment the ink arrives at the surface and lasted until the gloss of the ink reached an equilibrium value. Ink was applied on the surface with a glass capillary tube, using the ejector principle, and the ink formed an even layer on the paper surface. The light

source was a laser (wavelength = 633 nm). The detector part in the DIGAT apparatus measures the voltage from the glossmeter as a function of time. The laser beam and the detector were both fixed at an angle of 20° to the horizontal surface. The results are given in terms of absorption time corresponding to the time between 90% of the maximum gloss value and 10% of the equilibrium liquid saturation gloss value. In this measurement, the ink was an anionic aqueous dye-based ink from a Versamark VX5000e high-speed inkjet press. The applied ink amount in the device was 8 gm^{-2} .

The inkjet ink penetration in the coating layers and base paper was studied with a capacitance-based device, as shown in Figure 1. The measuring principle is based on the fact that the resistivity of a dry surface is very high, whereas a moistened paper and inkjet ink conduct electricity. The liquid, therefore, forms a conducting material whose movement affects the capacitance between the liquid chamber above and an electrode beneath the studied sample. Figure 1 (right side) shows a schematic illustration of how the Clara device works. The chamber can be pressurized from -0.5 to $+5$ bar, which allows a pressure to be generated for the ink-transfer region that is similar to what might occur due to the impact of the ink droplet in actual inkjet printing. Although this pressure refers to impact only, it is probably one factor that initiates wetting. Its continued presence has an effect on the penetration. The measuring area was 6.8 cm^2 . The area over which the applied liquid covered the sample surface was clearly larger than the detection area, and therefore, the wetted area next to the detection area limited sideways liquid motion. The level of capacitance to be measured was preadjusted to be on the correct expected level, derived from experience, in order to maximize sensitivity.

To evaluate the relation between the penetration depth and the capacitance value, a further experiment was made using coating filtercakes of PCC and PCC with 7 pph SA latex (thickness 294–540 μm) into which different amounts of molten candle wax, containing a colorant for ease of observation, had been allowed to absorb. The wax partially filled the porosity of the coating structure and, therefore, simulated the liquid front at a certain depth within the sample. Wax has a capacitance similar to that of the relative highly porous inkjet PCC coating, and importantly, it has a capacitance greater than air. Thus, as air is replaced by wax in the coating structure, provided that the wax does not interfere with skeletal connectivity, the capacitance would be expected to rise. The capacitances (averages of results between 1 and 1000 Hz) and the wax imbibition distances (relative distance = wax distance divided with the sample

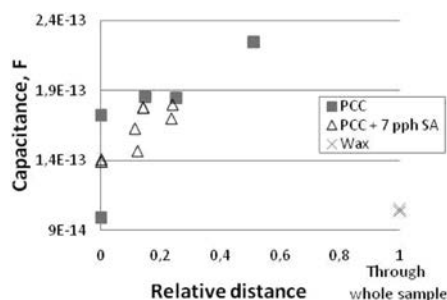


Figure 2. Connection between relative distance and capacitance determined using molten candle wax, containing a colorant for ease of observation, imbibed into coating filtercake structures. The samples were PCC and PCC with 7 ppH SA latex cakes.

thickness) were measured. As the depth of wax increased, higher capacitances were observed (Figure 2). (Note that, in this case, we could not use the original Clara capacitance-based device because the samples were too small for the detector. Therefore, we used a device that had a round electrode with a 5-mm diameter.) The device produced a reference value for the dielectric constant of plain candle wax, similar to, for example, those of polyethylene and Teflon, which have dielectric constants of about 2.25 and 2.1, respectively. The action, therefore, was confirmed to be that of wax replacing air in the coating structure, as wax has a higher dielectric constant (~ 2) than air (~ 1).

It can be imagined that a deviation from this increase in capacitance could occur if the skeletal connectivity of the porous structure were disrupted by the uptake of the dielectric material and that the connectivity itself would contribute to the dielectric properties. However, a polar liquid (i.e., water in inkjet ink) increases the conductivity of the sample markedly more than such a change could manifest itself, so that the capacitance method can be considered valid for the uptake of conductive liquids.

Before the actual sample measurement, the capacitance of a plastic film, used as a fixed-point backing, was evaluated and recorded; it was found to be approximately 190 pF. The sample testing was then started. First, the liquid was applied to the chamber and pressurized. The capacitance measurement started when the removable plate was taken away and the liquid started to penetrate the substrate. The plate had to move for 3.8 ms before it had moved away from the detection area. The capacitance was measured at 1-ms intervals. The liquid amount applied was clearly higher than that used in actual inkjet printing, and the pressure had an effect throughout the measurement time. The final result was a curve of capacitance change over time, and each sample was measured five times in parallel. In practice, an external pressure of 0.1 bar was used as representative of the internal pressure caused by the impact of the inkjet droplets. This corresponds to an inkjet ink droplet with a size of 15 pL (used in Versamark VX5000e high-speed inkjet press) flying with a velocity of 15 m s^{-1} causing about 0.1 bar of pressure on the surface. The dye-based cyan ink, from the Versamark VX5000e set, expressed a surface tension of 52.8 mN m^{-1} at 25°C and a viscosity of 1.1 mPas. In the inkjet printing, the pressure that the droplet impact causes to the paper surface is only initially present. In the Clara experiment, the external pressure affected the entire measuring time, even after the initial wetting. However, the

pressure was relatively small compared to the pressure of capillaries. The amount of ink applied was 5 cm^3 to provide an initial supersource. Some disturbances could appear in the results during the first few milliseconds in time because of the plate movement, and the area over which the ink made contact with the coating layer increased during the plate movement as well. To ensure similarity between the curtain-coated surfaces on precoated base paper and the pure coating structure on plastic film, a corresponding plastic film layer was placed behind the paper samples. The Clara device was also operated during a second measurement regime under a negative pressure (-0.1 bar). The aim of this experiment was to reduce the impact of externally driven permeability, such that capillarity acted initially to fill pores and, subsequently, the air permeation due to the negative pressure led to an equilibration of the wetting front.

If the thickness of the coated paper is known, one can calculate the penetration speed, assuming that the liquid has penetrated through the entire available structure behind the wetting front. This approximation is equivalent to the so-called Darcy approximation of length penetrated as a function of volume and filled porosity. That it is not the case was predicted by the work of Ridgway et al.⁴ and the experimental work of Gane and Koivunen.²³ Nonetheless, it is a representative average approximation. The paper thickness, d_{paper} , in the z direction, can be divided into two parts: the thickness of the wet sample, $d_{\text{wet}}(t)$, and that of the dry sample, $d_{\text{dry}}(t)$.

$$d_{\text{paper}} = d_{\text{dry}}(t) + d_{\text{wet}}(t) \quad (3)$$

The wet part contains ink, and this increases the capacitance values. The total capacitance, C_{tot} is the capacitive impedance series sum of the plastic capacitance, C_{pl} , coming from the plastic sheet under the sample and the sample capacitance, $C(t)$

$$\frac{1}{C_{\text{tot}}} = \frac{1}{C(t)} + \frac{1}{C_{\text{pl}}} \quad (4)$$

The total wetted paper has practically no impedance (pure conductor), and thus, the capacitance depends on the thickness of the dry paper

$$C(t) = \frac{A\varepsilon(\omega)}{d_{\text{dry}}(t)} \Rightarrow d_{\text{dry}}(t) = \frac{A\varepsilon(\omega)}{C(t)} \quad (5)$$

where A is the area and $\varepsilon(\omega)$ is the dielectric permittivity of the dry material at frequency ω . The permeability can be further expressed as the product $\varepsilon(\omega) = \varepsilon_0\varepsilon_r$ of the vacuum permittivity ε_0 and the relative permittivity of the material ε_r . At the end of the measurement, when the whole paper has been wetted, the paper has no impedance ($= 1/\text{capacitance}$). Thus, the plastic capacitance can be estimated to be the total capacitance at the end of the measurement [$C_{\text{pl}} = C(t=\infty)$].

The thickness of the wet part of the paper, which we estimate to be the penetration depth of the water front, can be calculated by combining eqs 3–5

$$d_{\text{wet}}(t) = d_{\text{paper}} - \frac{A\varepsilon(\omega)}{C(t)} = d_{\text{paper}} - A\varepsilon(\omega) \left(\frac{1}{C_{\text{tot}}} - \frac{1}{C_{\text{pl}}} \right) \quad (6)$$

Table 2. Porosity of Speciality PCC and Standard GCC Coating Cakes Measured with Silicon Oil Absorption

sample	Si oil porosity (%)
PCC 7 pph PVOH	48.3 ± 0.1
PCC 15 pph PVOH	37.0 ± 0.3
GCC 7 pph PVOH	39.1 ± 0.2
GCC 15 pph PVOH	21.5 ± 5.4

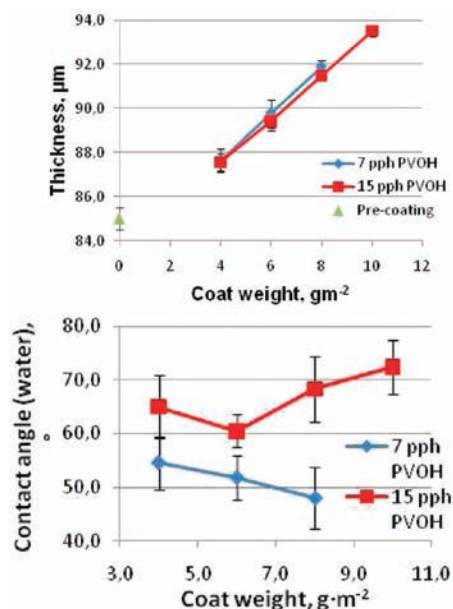


Figure 3. Thickness (top) and contact angle (water at 0.1 s, bottom) of PCC-coated papers.

The final $d_{\text{wet}}(t)$ equation used is

$$d_{\text{wet}}(t) = d_{\text{paper}} \left[1 - \frac{\frac{1}{C_{\text{tot}}(t)} - \frac{1}{C_{\text{tot}}(t = \infty)}}{\frac{1}{C_{\text{tot}}(t = 0)} - \frac{1}{C_{\text{tot}}(t = \infty)}} \right] \quad (7)$$

4. RESULTS

4.1. Intrinsic Properties of Coating Layers Measured on Plastic Film. Table 2 lists the results of Si-oil porosity measurements for the inkjet specialty PCC and offset standard GCC coating layers. The inkjet specialty PCC coatings, as expected, had higher porosities than the offset standard GCC coatings at comparable PVOH binder doses. Our previous study,²⁴ in which we used the same pigments with 10 pph of the same PVOH binder, also showed that the specialty PCC coating not only produces a coating layer with a higher pore volume but also displays a significantly greater pore volume associated with the smaller-diameter pores (20–70 nm) than the standard GCC

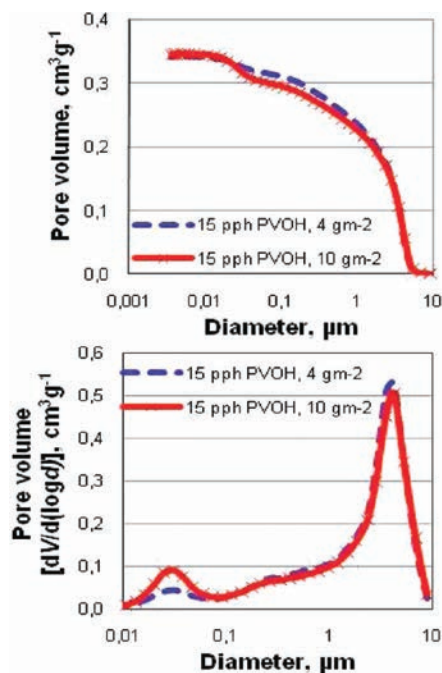


Figure 4. Cumulative pore volume (top) and first derivative of the pore size distribution (bottom) of inkjet PCC with 15 pph PVOH coatings with 4 and 10 gm⁻² coat weight on standard pre-coated paper, measured by mercury porosimetry.

coating. The GCC coating, in contrast, has more specific pore volume in the range of 0.1–0.3 μm.

4.2. Basic Properties of Curtain-Coated Papers with Specialty Inkjet PCC. The thicknesses of curtain-coated papers are illustrated in Figure 3. At a defined coat weight, the 7 and 15 pph PVOH specialty PCC-coated papers had very similar thicknesses, and a link exists between the pore volume and coating thickness for these coatings. Figure 4 shows how the 10 gm⁻² coating provided a higher specific pore volume to the coated paper than the 4 gm⁻² coating. In addition, the 10 gm⁻² coating structure had slightly less pore volume associated with pore diameters of >1 μm, whereas it had more 20–60-nm-diameter pores. Importantly, there appears to be no difference in the characteristics of the pore size distributions; that is, no additional peaks occurred to differentiate between the coat weights to suggest any major changes in coating structure. This effect on specific pore volume size distribution, therefore, closely represents the proportion of specialty coating in relation to the total paper.

The contact angle of water (at 0.1 s) in equilibrium is seen in Figure 3. Both the 7 and 15 pph PVOH coatings were hydrophilic, and the 7 pph PVOH-containing coatings provided lower contact angles than the 15 pph PVOH coatings. It seems that the 15 pph PVOH-containing coatings were, therefore, less hydrophilic than the 7 pph PVOH-containing coatings, although binder swelling might act as a pinning mechanism. Furthermore, the roughness of the 7 pph PVOH coatings was on the level of 90 mL min⁻¹ (Bendtsen), whereas that of the 15 pph PVOH

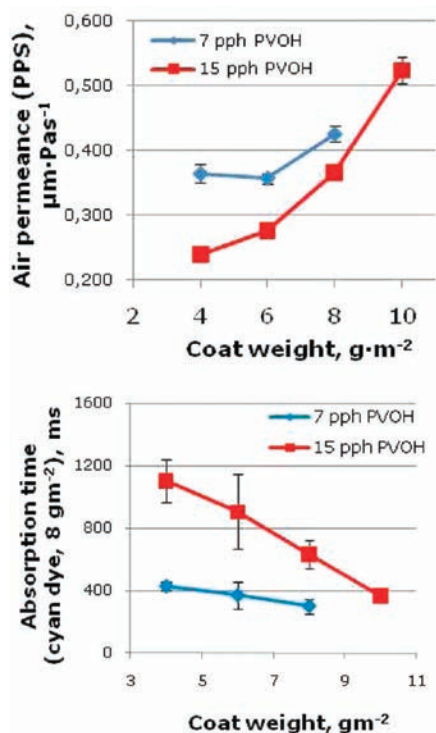


Figure 5. Apparent air permeance (top) and ink absorption speed (bottom, DIGAT device, dye-base ink amount 8 gm^{-2}) of specialty inkjet PCC-coated papers.

coatings was 120 mL min^{-1} , and this might be an additional reason for the contact angle difference.

The air permeance results for the specialty inkjet coatings are shown in Figure 5 (top). The higher the coat weight, the greater the apparent air permeance. This result is different from the results of Xiang and Bousfield,¹⁴ who studied offset coatings. The difference is directly due to the measurement technique and its relation to the paper structure. Air permeance is measured by applying an external pressure to force air through the paper sheet. It is, however, not a suitable method for determining the permeability of layered structures where, for example, a significant coat weight of a more permeable layer is applied on top of a less permeable layer. In this case, the precoat forms a less permeable layer than that generated by the specialty inkjet coating. Instead of passing through the complete sheet, the air is directed by preferential permeability laterally through the more permeable top layer, escaping proportionally to the sides of the sample. Thus, as coat weight increases, so do the effective permeation radius and escape path length (eq 1), and one can see, in Figure 5 (top), that the effect is therefore exponential as a function of coat weight.

The absorption speeds of 7 pph PVOH coatings were very near each other (Figure 5, bottom), being only slightly dependent on coat weight. The 15 pph PVOH coatings, however, although exhibiting slower absorbance than the lower-binder-level coatings at low coat weights, gradually absorbed more

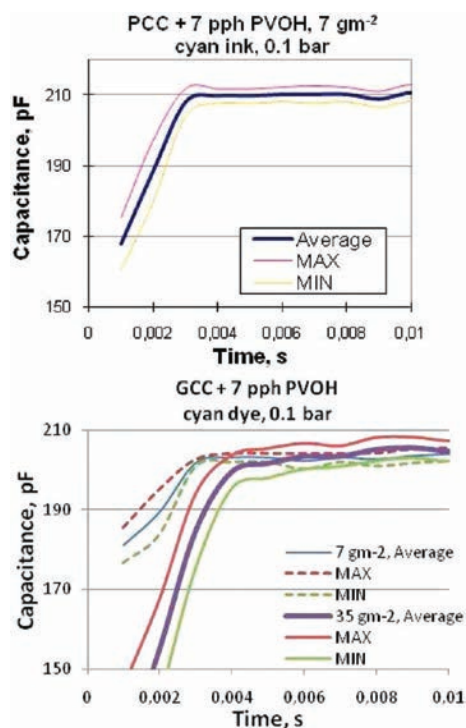


Figure 6. Two examples of the average and confidence interval of results from coatings during Clara measurements. The examples are from the inkjet specialty PCC coating containing 7 pph PVOH and the standard offset GCC with 7 pph PVOH on the plastic film surface. The ink was dye-based cyan ink, and the measuring pressure was 0.1 bar.

rapidly as the coat weight increased, approaching the speeds of the lower-binder-level coating at the highest coat weights. This behavior reflects the relative total porosities of the coating layers, which are the sums of the available pore volumes per unit area of liquid contact. This pore volume available for absorption is controlled by binder level (more binder reduces it) and coat weight (higher coat weight increases it). That the two coating structure types have absorption rates that approach each other asymptotically at higher weights shows that the final absorption rate is determined by permeability once sufficient pore volume is present. All of these results show that the structures of the coating layers differ from each other mainly as a function of binder level. The function of coat weight relates primarily to the total available pore volume for a given binder dose. Thus, at this stage, it is possible to state that the differences are due mainly to the structural changes in the total sheet as the coat weight of the specialty layer changes (i.e., they are related primarily to the topcoat/precoat ratio). The presence of a higher dose of PVOH clearly plays the major role in reducing the absorption efficiency by limiting the available pore volume per unit absorption time, and because PVOH itself absorbs water by interpolymer network diffusion, this dependence most likely is manifested as one of diffusion rate.

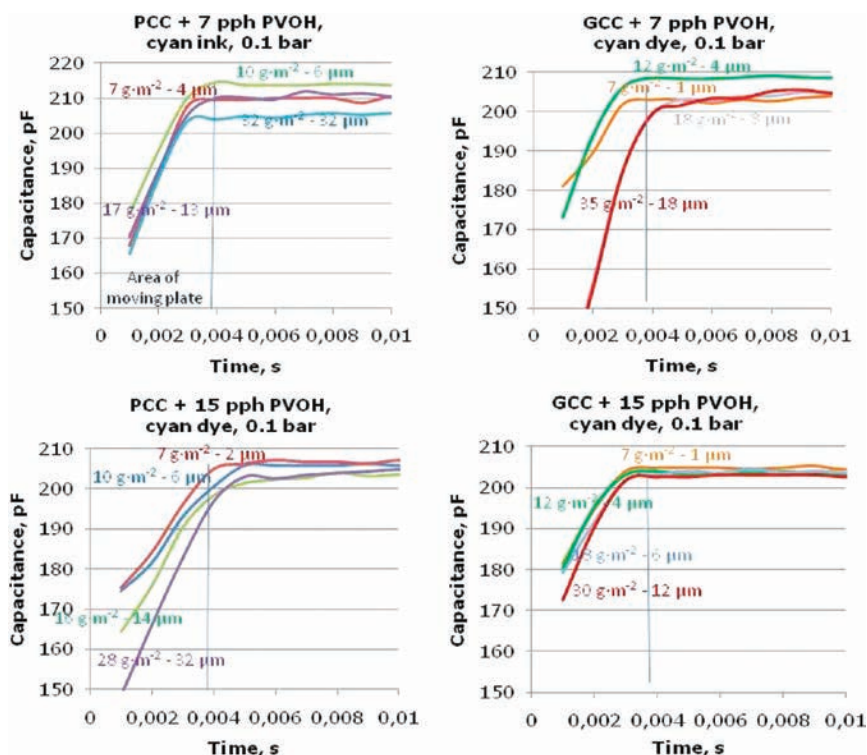


Figure 7. Effect of coating layer thickness on capacitance (Clara). The inkjet specialty PCC and offset standard GCC coatings in this case were on plastic film. The thickness of each coating layer was added after the coat weight value. The ink was cyan dye-based ink from a Versamark VX5000e inkjet press. The final capacitance level of Clara results was found to depend on the variation of the used plastic film (204–212 pF).

4.3. Clara Liquid Permeation Measurements. Coating Layers on Impermeable Film. The reproducibility of the results from the Clara capacitance device can be seen in the examples shown in Figure 6. One can, with confidence, differentiate the results of different coating thicknesses in the case of the GCC coatings, as they lie well outside the limits of variation. From this finding, one can assume that, if the results for different coatings appear similar to each other, despite differences in coat weight, then the liquid transport properties are the same, as in the case of specialty PCC coating containing 7 pph PVOH (Figure 7).

Figure 7 shows, first, that the inkjet specialty PCC coating provided thicker coating layers than the offset standard GCC coating at an equivalent coat weight. The GCC pigment forms a more tightly packed coating layer structure, as indicated by the Si-oil porosity results.

We expect that the ink would penetrate through the thinner coating layer in a shorter time than it would penetrate through the thicker one, and this is evident in the results of the Clara device. Figure 7 shows how the cyan dye-based ink penetrated very quickly through the whole of the applied coating layers at 0.1 bar of external pressure. Most of the result curves reached the maximum value of capacitance during a time of 0.004 s. The removable plate transferred out of the measuring area during the first 0.0038 s, and therefore, the results of the first millisecond of time are highly affected by the plate removal, as well as the fact that the detection area was not yet completely covered with ink.

Thus, one must remember that the results are reliable when using the Clara device only after 0.0038 s. If the results of the first milliseconds in time are studied more closely, it seems that higher coat weights on the film were associated with lower locations of the starting point of the capacitance curve. The lower starting point difference relates to the absorption occurring nonuniformly during the removal of the covering plate. The correspondence to the inverse relation of capacitance with sample thickness is taken into account in the measurement, and therefore, the relative capacitances reflect structural/compositional differences with respect to the dielectric constant of the medium created. Once again, this relates to the increasing portion of the specialty layer as a function of coat weight.

The capacitance results of specialty PCC coating layers exposed to liquid ink on the plastic film under the influence of negative pressure (–0.1 bar vacuum) are illustrated in Figure 8. The capacitance was highest in the beginning of the measurement, and it decreased over time, indicating the removal of liquid from the permeation-controlling pore structure.

Curtain-Coated Papers. The reproducibility of coated paper results is illustrated in Figure 9. There was no significant variation in the results from repeated measurements on fresh samples from a single example coated paper, indicating that the paper had a uniform structure and that the measurement was reproducible.

The inkjet coatings applied to the precoated paper were studied first with an external pressure of 0.1 bar to measure

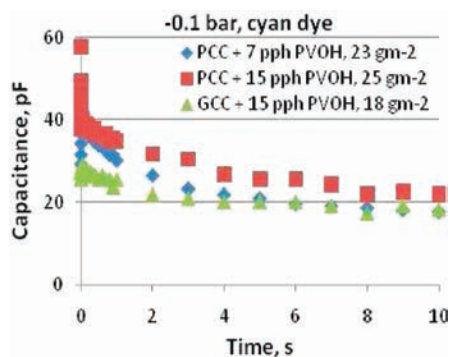


Figure 8. Capacitance results of cyan ink under the influence of -0.1 bar vacuum. The inkjet specialty PCC and offset standard GCC coatings in this case were on the plastic film. The ink was cyan dye-based ink from a Versamark VX5000e inkjet press. The final capacitance level of Clara results depends on the variation of used plastic film (18–22 pF).

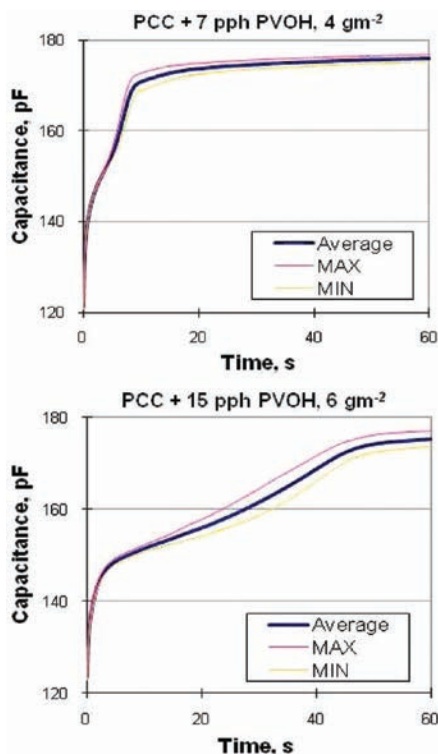


Figure 9. Two examples of the average and confidence interval of inkjet specialty PCC-coated papers measured with the Clara device. The average, minimum, and maximum values were calculated from the results of five parallel measurements of each sample.

liquid permeation. The bimodal behavior of each curve (Figure 10) illustrates the competition between the initial capillary wetting and the permeable flow characteristic once

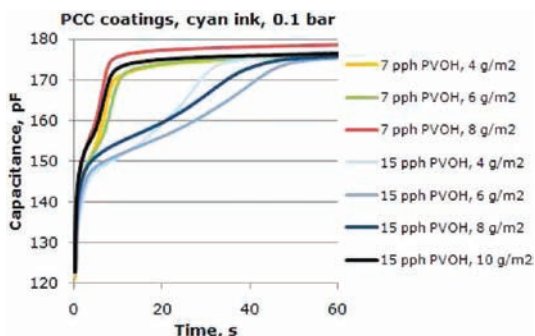


Figure 10. Effect of coat weight on the penetration of cyan inkjet ink in the inkjet specialty PCC coatings that contained 7 and 15 pph of PVOH. The external pressure of the Clara measurement was 0.1 bar.

the capillaries/pores are filled. At equivalent coat weights, the 15 pph PVOH coatings exhibited longer liquid penetration times through the sample than the 7 pph PVOH coatings. The ink penetration through the structure of the 7 pph PVOH coatings took from 7.5 to 11 s, and that through the 15 pph PVOH coatings took from 8 to 50 s. Thus, a higher amount of PVOH decreased the coating layer porosity and permeability. Therefore, it took more time for ink to penetrate through the coating layer, and because the permeability was reduced, it took longer to force liquid through the top layer into the substrate. Additionally, a higher PVOH amount likely leads to more migration of the PVOH into the underlying structure.

From the air permeance point of view, the 7 pph PVOH coatings with 4 and 6 gm^{-2} and the 15 pph PVOH coating with 8 gm^{-2} were very similar. The capacitance-based results were partly in harmony with these results, especially during the first second. However, the data points after 1 s diverged and the ink went through the 15 pph PVOH coating surfaces slower than through the 7 pph PVOH coatings. The results of DIGAT device showed a similar difference. On the other hand, the capacitance and DIGAT results were very similar in the case of the 8 gm^{-2} 7 pph PVOH coating and the 10 gm^{-2} 15 pph PVOH coating, but the air permeance of the 15 pph coating was higher because of the greater lateral cross section associated with its increased coat weight.

5. DISCUSSION

5.1. Ink Penetration in Coating Layers on Film. The results in Figure 7 show that inkjet ink from the applied supersource volume more or less penetrates through the coating layer, even though it is up to 35 μm thick, during 0.004 s of time at an external pressure 0.1 bar, and all resulting curves look very similar regardless of the coating pigment type, the binder amount, or the thickness of the coating layer. It seems that capillary absorption in the coatings occurs on a time scale equal to or shorter than 0.004 s. In contrast, for time delays longer than 0.004 s, permeation flow dominates in the coating structures. These results agree very well with the results of Ridgway et al.^{4,25} With a Pore–Core computer model of void structure, they calculated how quickly alcohols and water move in the coating layer structure. They concluded that smaller-radius capillaries initially fill faster than larger ones. The fine capillaries were found to fill faster until 0.00026 to 0.00056 s,

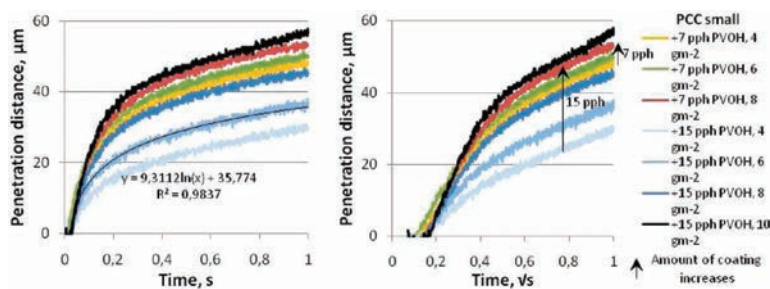


Figure 11. Penetration distance of dye-based ink in the inkjet specialty PCC coatings as a function of time and square root of time, respectively, clearly showing the two regimes of absorption, measured with the Clara device at a pressure of 0.1 bar using cyan dye-based ink.

depending on the equation used, and after this time, the larger capillaries started to fill at a higher rate.

The results indicate that the capillary flow of the coating layer is too fast for the Clara device. Using the Bosanquet absorption equation,²⁶ which takes into account the inertial flow of liquid, the speed of absorption into a 0.1- μm -length pore is below 10 ns.⁴ However, the Clara device starts the detection at 1 ms. This means that the coating passed by the first preferred-pathway wetting front in an idealized free-access structure (nonpermeability limited) is about the scale of 1 cm. The maximum coating thickness used was 32 μm , which, because the network is complex, probably does not exhibit centimeter-scale pathways for ink, but is highly likely to have been traversed completely by the ink meniscus front in this relatively long time scale in absorption terms.

The starting points of capacitance curves (Figure 7) seemed to be located at lower levels when the coat weight was increased. This means that thicker coating layers had more open pore volume during the first few milliseconds of absorption than thinner ones. However, one must remember that, during the first 0.0038 s of time, the detected area was still increasing because of the plate movement during removal. The area increased during this time, and the ink transferred deeper into the coating layer of the starting edge than near the plate edge. Nonetheless, this provides more likely evidence for the preferred-pathway wetting phenomenon, described by Ridgway et al.,^{4,25} as a greater proportion of pores are initially bypassed as the length of the sample increases.

The capacitance results under a vacuum indicate that, at first, the ink penetrates some way into the coating structure, and therefore, the highest capacitances occur during the first 0.007 s. Then, the absorbed liquid retracts and saturates to the level of 18–22 pF. This suggests that a migration of liquid occurs after the first capillary absorption as the pore structure fills ever closer to the wetting front, forming a nonpermeable liquid layer that then gets drawn under the negative pressure to the top surface. The PVOH-containing coatings have a hydrophilic and hygroscopic nature, and therefore, the capillary rise depends on the bulk concentration of surfactants in the ink and the surface tension of the liquid/vapor interface that has already developed at the contact with the capillary.¹² Additionally, the water diffuses rapidly into the PVOH polymer network. It seems that these PVOH swelling forces lead to a closure of air permeability, so that the ink is effectively forming a mobile but impermeable barrier within the coating that is forced back to the surface layer of the coating by the negative pressure of the vacuum. A strong positive

capillary pressure is therefore required before the liquid starts to equilibrate again in the capillaries.

5.2. Ink Penetration in Curtain-Topcoated Papers. Figure 11 shows how the penetration distance of dye-based ink develops differently depending on coating layer structure and, thus, especially in 15 pph PVOH-containing coatings. In general, the ink penetrates deeper in a given time when the paper has a higher ink absorption speed. The 7 pph PVOH-containing coatings were quite similar, and the curves of ink penetration were located very near each other. At equivalent coat weights, the ink has penetrated less into the coating structure containing 15 pph PVOH than into that containing 7 pph PVOH. Figure 11 illustrates that, in the beginning of the absorption into the specialty inkjet coated paper, the penetration distance results have quite a linear relation to the square root of time, indicating either equilibrated Poiseuille laminar flow according to the long-time-scale-applicable Lucas–Washburn equation and/or a Fick's law diffusion response. However, there seem to be two linear regions with respect to the square root of time during the first second: the first from the beginning to a time of 0.2 s and the second from 0.2 s onward (Figure 11). This result agrees with the results of the study of PVOH-containing coatings reported by Ström et al.² In the first linear region, the properties of the coating layer structure predominantly affect how the ink will move there, and in the second region, the porous structure of the base paper influences how the ink moves. This turning point seems to be located at a distance of 15–35 μm into the coating, depending on the coating layer thickness. The thicknesses of the applied curtain-coating layers were between 2.5 and 8.5 μm (Figure 3). It was impossible to measure the thickness of the precoat layer directly, but it seems that the turning point was located neither in the precoat layer nor just under it. The turning point was located deeper within the base paper. This suggests either that the fiber base paper is effectively a zero-resistance layer in comparison to the coating structures or that the poly(vinyl alcohol) has also penetrated deeply, rendering the diffusion effect active throughout the sheet. If the external pressure had been lower, then the role of diffusion would have been even higher. In the coating layer immobilization process, PVOH can penetrate into the deeper areas of the paper structure, thereby affecting the porosity of the top layer of base paper, effectively making it a continuation of the coating itself. On the other hand, PVOH swells under the influence of water-based ink, which will act to close the smallest pores and diminish the pore diameters during the ink penetration. PVOH can also dissolve partially into the inkjet ink during the penetration process,

thereby affecting the liquid properties. The precoating penetration into the base paper could be a further reason. This result suggests that, in the structure of swelling PVOH, the movement of ink after the first capillary-driven absorption follows a diffusion rate according to the PVOH liquid uptake. In parallel, the longer-time-scale absorption becomes permeability-limited, and so, as the relevant short-time-scale equations of Bosanquet and Szekeley predict, the mechanism collapses back into equilibrium-viscosity-controlled flow.

If the results on coated plastic film and those for the same coating color on the paper surface are compared, one can notice that, on the paper surface, at 0.05 s, the ink has penetrated a distance of $8.5 \mu\text{m}$, whereas on the plastic film coating, it took only 0.004 s to penetrate a $32\text{-}\mu\text{m}$ -thick coating. In the case of the coating layer on the plastic film, there is more or less a single well-defined pore size distribution and porosity, which provides a system wherein the ink moves more or less uniformly at the same rate through the coating layer. Furthermore, on plastic, all applied coating components are located in the coating layer. On paper, the coating layer is less uniform, and there are permeable regions where the liquid can be forced under pressure through the coating into the substrate pore structure, delaying the effective penetration into the neighboring intact coating structure. With respect to imbibition mechanisms, the capillary flow is first active in the finest pores, and once these surface capillaries become saturated, the permeability becomes the controlling factor for further imbibition. When coated on plastic, the ink, once having penetrated through the coating layer, can spread only in the coating layer edge structure areas because of the nonpermeable nature of the film. In the case of coated papers, the structure contains different layers, namely, the topcoat, the precoat, and ultimately the base paper, with very different pore-size distributions and porosities. The PVOH applied in the topcoat layer can be partially located in the precoating and/or the base paper, and therefore, the ink does not proceed at the same rate through the whole structure. The coating layer has more fine pores than the base paper, and therefore, the ink transfer is faster with respect to pore-filling rate. In the case of polar inkjet ink, the diffusion into the hydrophilic matrix of both the coating layer and the base paper affects the ink movement dynamic by changing the effective small capillary diameters, where the swelling polymer is located and, hence, the uptake amounts in these structures during measurements. We can conclude that capillary flow dominates in the coating layer on plastic, but in the case of coated paper, which has only a 10 gm^{-2} coating, it is hard to see the capillary effect with the Clara measurement while permeation dominates. Permeation flow and diffusion, therefore, dominate with respect to volume imbibition when lightweight coatings are applied to paper.

Figure 12 shows how the penetration speed into the specialty coated paper decreased in the coated paper structures when the ink moved deeper into the layer. The penetration front curves of 7 pph PVOH-containing coatings are very near each other, and the coat weight differences in the coatings had very minimal effect on the penetration speed, suggesting that the coatings have very similar structures and are not permeation-limited, such that the coating layer thickness has a very small impact on the speed of ink penetration in the 7 pph PVOH-containing coating layers. On the other hand, in the 15 pph PVOH-containing coatings, there was clearly a greater difference in the apparent air permeance, related to the increased lateral cross-sectional area for air escape balanced by the increased binder dose, and in the

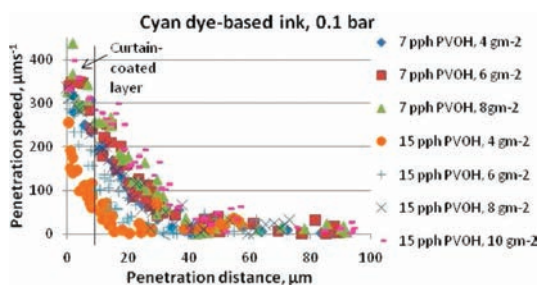


Figure 12. Penetration speed of commercial cyan ink at the different layer depths in specialty inkjet pigment topcoated paper, having a standard offset precoat and woodfree base paper, measured with the Clara device using cyan dye-based ink at an external pressure of 0.1 bar.

absorption speed. This could be readily detected in the Clara capacitance results. The ink penetrated with higher speed in the thicker coating layer, showing that it was pore-capacity-limited because of the extra binder. No unambiguous connection was found between the results for the contact angle of water and penetration speed in the coating layer. The reason might be in the contact angle measurement itself, where the coated surfaces had different roughness levels, but also in terms of the dominance of structural effects. The results at coat weights of 4 and 6 gm^{-2} , however, did indicate that a lower contact angle results in faster inkjet ink absorption, as might be expected.

Ridgway et al.⁴ indicated that the coating structure has an optimal aspect ratio for the fastest filling of liquid into individual pores, and the optimum seems to be located in the range $0.1 < l/r < 10$, where l is the length and r is the radius of the pores. For pores of 30-nm diameter, this means that the length of the pores in the optimal range is between 3 and 300 nm. One might expect to have this type of pores in the lowest-coat weight structure, too (i.e., at a coat weight where the connectivity is not yet fully established, so that the longer-term flow is not permeability-limited in the specialty layer). The mercury porosimeter results indicated that the specialty coating with 15 pph PVOH at a coat weight of 4 gm^{-2} had a smaller volume of 30 nm size pores than did the 15 pph PVOH coating at the higher weight of 10 gm^{-2} . In the case of 500-nm-diameter pores, the specific pore volume values spanning from 50 nm to $5 \mu\text{m}$ indicate that the low-coat-weight coatings with $2.5 \mu\text{m}$ thickness can hardly work in the fastest filling area. To achieve the fastest filling area by means of large-pore-diameter coatings, the thickness of the coating layer should be greater. By planning the coating layer so that there are small enough pores, one can also decrease the coating layer thickness and still reach the fastest ink penetration into the structure. The limitation then comes with respect to the underlying layers and the role of binder.

5.3. Effect of Ink Permeation on Intercolor Bleeding and the Final Print Quality. The structural properties of the coating reflect the ink tendency for intercolor bleeding during the ink setting process. Figure 13 shows online images of figures from Versamark VX5000e printing just after the print heads. The images illustrate how the coat weight and the printing speed affect the black ink intermixing with the cyan on the surface. All of the images show wicking paths where the black ink has moved into the area of the cyan color. The narrowest, most uniform black line was reached with the highest coat weight of specialty

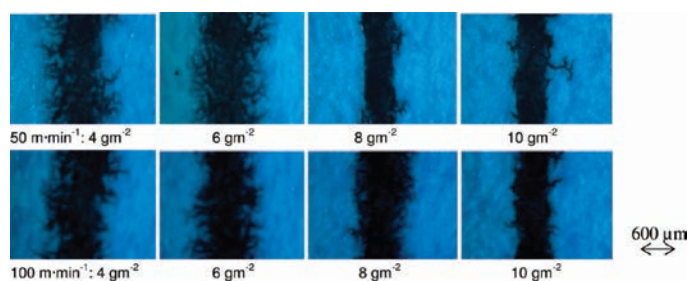


Figure 13. Online images of intercolor bleeding from specialty coatings that contained 15 pph PVOH using different printing speeds. The time delays between cyan and the online camera system were 2.2 s (50 m min^{-1}) and 1.1 s (100 m min^{-1}). The time delays between cyan and black were 1.1 and 0.54 s depending on printing speed.

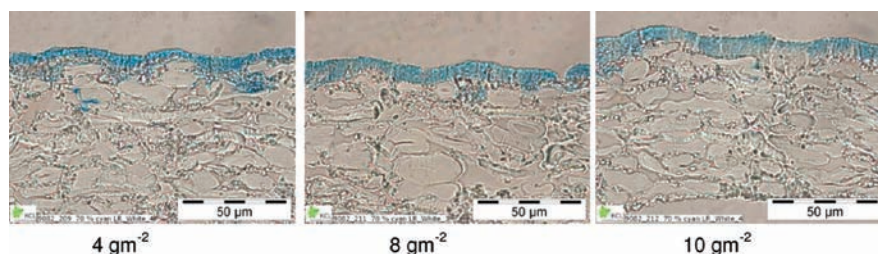


Figure 14. Cross-sectional images of printed 15 pph PVOH containing specialty coatings (70% half tone dot area). Coat weights of 4, 8, and 10 gm^{-2} .

inkjet surfaces. There was enough volume in these cases that the ink could penetrate quickly and sufficiently, that is, under conditions of the highest porosity with the highest penetration coefficient and the highest ink penetration speed.

The droplet speed of the Vesamark VX5000e inkjet press was 15 m s^{-1} , and the volume was 15 pL. The online images were detected on the 100% area at a resolution of $300 \times 300 \text{ dpi}$. Using these values, we obtain an ink amount of $2.09 \text{ cm}^3 \text{ m}^{-2}$ on the surface. Assuming that all coating layers had a total pore volume of $0.35 \text{ cm}^3 \text{ g}^{-1}$, which was almost the case of 15 pph PVOH-containing coatings, the 10 gm^{-2} coating would have a pore volume of $3.5 \text{ cm}^3 \text{ m}^{-2}$; the 8 gm^{-2} coating, $2.8 \text{ cm}^3 \text{ m}^{-2}$; the 6 gm^{-2} coating, $2.1 \text{ cm}^3 \text{ m}^{-2}$; and the 4 gm^{-2} coating, $1.4 \text{ cm}^3 \text{ m}^{-2}$. Thus, the applied ink can fill the coating structure completely when the coat weight is 6 gm^{-2} or below. In the Clara device, this total filled pore volume corresponds to a thickness of $4.5 \mu\text{m}$ at a time of 0.035 s.

An increase in the printing speed from 50 to 100 m min^{-1} (Figure 13) seemed to have a quite minimal effect on the intercolor mixing on the 15 pph PVOH inkjet coatings when the coat weight was low (i.e., 4 and 6 gm^{-2}). The black ink mixed with cyan already during the detection time delay 1.1 s (100 m min^{-1}). However, the 8 gm^{-2} papers produced a narrower, more uniform black line when a lower printing speed was used. The delays between the cyan and black nozzles decreased from 1.1 s (at 50 m min^{-1}) to 0.54 s (at 100 m min^{-1}), and it seems that the lower printing speed gave the cyan ink enough time to penetrate into the structure so that the black ink could not mix with it. The Clara and DIGAT results show also that the penetration speed of the ink increased as coat weight increased. From the color-mixing point of view, the penetration speed of the first color seems to have a very important role in the dye-based ink inkjet press. One

way to affect the intercolor mixing is to plan the location of the drying part carefully.

The online images of 7 pph PVOH-containing coatings (Figure 15 at a printing speed 50 m min^{-1}) look very similar to the images of 15 pph PVOH-containing coatings at 4 and 6 gm^{-2} . There were less noticeable differences between the coat weights or printing speeds (not shown herein).

Figure 14 shows the cyan colorant location in the coating layer after printing. It seems that the colorant is located more on the top part of the coating layer when the coat weight increases. It is probably the poly(vinyl alcohol) of the coating color that takes the colorant with the water into the polymer matrix. At the lowest coat weight, some of the colorant could also be detected in the base paper structure. It can also be seen that the coatings had cracks, probably related to the shrinkage of polymer in flocculating/immobilized structures during drying.

If the pore structure (pore volume and pore size distribution) of the coating layer were constant and the only variable were the thickness of the coating, a thicker coating layer would have more total pore volume into which the ink could penetrate. This means that, on a lower-coat-weight coating, the ink stays longer on the top of the coating layer because the ink first penetrates quickly into the small-pore-size fraction of the coating structure and the wetting front is pinned for a while at the interface between the absorption regimes of the small- and large-pore-size fractions, inertially delayed, before progressing into the underlying pre-coating. This result agrees well with the results of Svanholm.¹³ The longer the ink front remains pinned in the topcoating, the higher the probability that the inks will mix with each other. The 7 pph PVOH coatings at 4 and 6 gm^{-2} and 15 pph PVOH coating at 8 gm^{-2} had similar air permeance results. Figure 15 shows the inks mixing after 2.2 s (50 m min^{-1}) after the cyan ink printing.

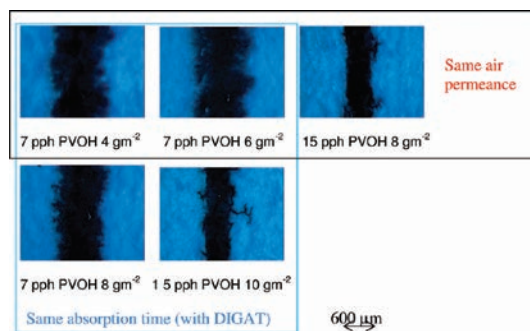


Figure 15. Inks mixing in coatings having the same air permeance and same absorption time but different coat weights. Online images at a printing speed of 50 m min^{-1} .

The highest coat weight produced the narrowest black line on the cyan surface, and there was less ink mixing. If the same absorption time is achieved in coatings with different thicknesses (Figure 15, 7 pph PVOH-containing coatings versus 15 pph PVOH-containing coatings with 10 gm^{-2}), one can notice again that the thicker coating layer provides a narrower black line and less ink mixing than the coating with the lower coating layer thickness. A higher coat weight coating has a higher volume into which the ink can penetrate.

These results collectively indicate that absorption speed is not the only criterion for preventing intercolor bleeding during inkjet ink drying. Rather, the combination of continuity of absorption over time coupled with sufficient total pore volume within the rapidly absorbing layer is key. The presence of diffusion-controlling binder is seen as a limiting factor to achieving optimal inkjet coatings at low coat weights in cases where the pore structure derived from the pigment alone is properly designed.

6. CONCLUSIONS

The penetration of dye-based inks in specialty inkjet coatings at the external pressure caused by the impact of inkjet ink droplets was studied with the capacitance-based Clara permeation device. The results measured from specialty coating layers on plastic film showed that permeation flow dominates in the coating layer only after at least 0.004 s after the application of the ink. Capillary flow, therefore, acts earlier in time than permeation. The pigment type, the binder amount, and the coating layer thickness were found to have no influence on these relative results.

The highest coat weight (10 gm^{-2}) of curtain-coated specialty inkjet surfaces produced the highest total paper porosity, the highest apparent air permeance, and hence the greatest pore volume. The thicker the coating layer, the higher the penetration speed. The highest coat weight also had the most 20–60 nm diameter pores relative to the total paper structure. All of these findings relate to the simple relationship between the topcoating proportion and the total sheet weight. Online images collected on the press show how inkjet inks mix together less when the coating layer has high air flow and high absorption speed. When surfaces with same air permeance or absorption speed are compared, the thicker coating layer produces less ink wicking and reduced intercolor bleeding. The printing speed affects the mixing of inks, as the speed influences the delays between the

different color nozzles, and higher coat weight provides greater pore volume.

In summary, the results indicate that absorption speed is not the only criterion for preventing intercolor bleeding during inkjet ink drying. Rather, the combination of continuity of absorption over time coupled with sufficient total pore volume within the rapidly absorbing layer is key. The only way to decrease the coat weight of specialty inkjet coating layers, therefore, is to use pigments that produce a structure with a high proportion of nanopores and a high permeability. The presence of a diffusion-controlling binder is seen as a limiting factor to achieving optimal inkjet coatings at low coat weights in the case where the pore structure derived from the pigment alone is properly designed.

AUTHOR INFORMATION

Corresponding Author

*E-mail: taina.lamminmaki@vtt.fi

REFERENCES

- (1) Donigian, D. W.; Wernett, P. C.; McFadden, M. G.; McKay, J. J. Ink jet Dye Fixation and Coating Pigments. Presented at the *TAPPI Coating/Papermakers Conference*, New Orleans, LA, May 4–6, 1998; Paper 12-3.
- (2) Ström, G. R.; Borg, J.; Svanholm, E. Short-Time Water Absorption by Model Coatings. Presented at the *TAPPI 10th Advanced Coating Fundamentals Symposium*, Montreal, Canada, Jun 11–13, 2008; Paper 19.
- (3) Nilsson, H.; Fogden, A. Inkjet Print Quality on Model Paper Coatings. *Appita J.* **2008**, *61*, 120.
- (4) Ridgway, C.; Gane, P. A. C.; Schoelkopf, J. Effect of Capillary Element Aspect Ratio on the Dynamic Imbibition within Porous Networks. *J. Colloid Interface Sci.* **2002**, *252*, 373.
- (5) Ridgway, C.; Gane, P. A. C. Controlling the Absorption Dynamic of Water-Based Ink into Porous Pigmented Coating Structures to Enhance Print Performance. *Nord. Pulp Pap. Res. J.* **2002**, *17*, 119.
- (6) Olsson, R.; van Stam, J.; Lestelius, M. Effects on Ink Setting in Flexographic Printing: Coating Polarity and Dot Gain. *Nord. Pulp Pap. Res. J.* **2006**, *21*, 569.
- (7) Ivutin, D.; Enomae, T.; Isogai, A. Ink Dot Formation in Coating Layer of Inkjet Paper with Modified Calcium Carbonate. Presented at the *NIP 21 International Conference on Digital Technology*, Baltimore, MD, Sep 18–23, 2005; Paper 119.
- (8) Ridgway, C.; Gane, P. A. C. Correlating Pore Size and Surface Chemistry during Absorption into a Dispersed Calcium Carbonate Network Structure. *Nord. Pulp Pap. Res. J.* **2006**, *21*, 563.
- (9) Schoelkopf, J.; Gane, P. A. C.; Ridgway, C. J.; Matthews, G. P. Practical Observation of Derivation from Lucas–Washburn Scaling in Porous Media. *Colloids Surf. A: Physicochem. Eng. Aspects* **2002**, *206*, 445.
- (10) Gane, P. A. C.; Ridgway, C. J. Rate of Absorption Studies of Flexographic Ink into Porous Structures: Relation to Dynamic Polymer Entrapment during Preferred Pathway Imbibitions. Presented at the *27th IARIGAI Research Conference: Advances in Paper and Board Performance*, Graz, Austria, Sep 10–13, 2000; Paper 2.1.
- (11) Lamminmäki, T.; Puukko, P. New Ink Absorption Method to Predict Inkjet Print Quality. Presented at the *34th IARIGAI International Research Conference: Advances in Printing and Media Technology*, Grenoble, France, Sep 9–12, 2007; Paper 25.
- (12) von Bahr, M.; Kizling, J.; Zhmud, B.; Tiberg, F. Spreading and Penetration of Aqueous Solutions and Water-Borne Inks in Contact with Paper and Model Substrates. Presented at the *27th IARIGAI Research Conference: Advances in Paper and Board Performance*, Graz, Austria, Sep 10–13, 2000; Paper 2.2.
- (13) Svanholm, E. Printability and Ink-Coating Interactions in Inkjet Printing. Ph.D. Dissertation, Karlstad University, Karlstad, Sweden, 2007.

- (14) Desie, G.; Van Roost, C. Validation of Ink Media Interaction Mechanisms for Dye and Pigment-based Aqueous and Solvent Inks. *J. Imag. Sci. Technol.* **2006**, *50*, 294.
- (15) Walther, M.; Ortner, A.; Meier, H.; Löffelmann, U.; Smith, P. J.; Korvink, J. G. Terahertz Metamaterials Fabricated by Inkjet Printing. *Appl. Phys. Lett.* **2009**, *95*, 251107.
- (16) Haverinen, H. M.; Myllylä, R. A.; Jabbour, G. E. Inkjet Printing of Light Emitting Dots. *Appl. Phys. Lett.* **2009**, *94*, 073108.
- (17) Quéré, D. Inertial Capillarity. *Europhys. Lett.* **1997**, *39*, 533.
- (18) Zhumd, B.; Tiberg, F.; Hallstenson, K. Dynamics of Capillary Rise. *J. Colloid Interface Sci.* **2000**, *228*, 263.
- (19) Xiang, Y.; Bousfield, D. W. Effect of Coat Weight and Drying Condition Structure and Ink Setting. Presented at the TAPPI Advanced Coating Fundamentals Symposium, San Diego, CA, May 4–5, 2001; Paper 1-3.
- (20) Glittenberg, D.; Voigt, A.; Donigian, D. Novel Pigment–Starch Combination for Online and Offline Coating of High-Quality Inkjet Papers. *Pap. Technol.* **2003**, *44*, 36.
- (21) Lamminmäki, T.; Kettle, J.; Puukko, P.; Ketoja, J.; Gane, P. The Role of Binder Type in Defining Inkjet Print Quality. Presented at the *PTS Coating Symposium*, Baden-Baden, Germany, Sep 22–25, 2009; Paper 15.
- (22) Gane, P. A. C.; Kettle, J. P.; Matthews, G. P.; Ridgway, C. J. Void Space Structure of Compressible Polymer Spheres and Consolidated Calcium Carbonate Paper-Coating Formulations. *Ind. Eng. Chem. Res.* **1996**, *35*, 1753.
- (23) Gane, P. A. C.; Koivunen, K. Relating Liquid Location as a Function of Contact Time Within a Porous Coating Structure to Optical Reflectance. *Transport Porous Media* **2010**, *84*, 587.
- (24) Lamminmäki, T.; Kettle, J.; Puukko, P.; Gane, P. A. C.; Ridgway, C. Inkjet Print Quality: The Role of Polyvinyl Alcohol in Specialty CaCO₃ Coatings. Presented at the *7th International Paper and Coating Chemistry Symposium*, Hamilton, Ontario, Canada, Jun 10–12, 2009; Paper 49.
- (25) Ridgway, C.; Schoelkopf, J.; Matthews, G. P.; Gane, P. A. C.; James, P. W. The Effect of Void Geometry and Contact Angle on the Absorption of Liquids into Porous Carbonate Structure. *J. Colloid Interface Sci.* **2001**, *239*, 417.
- (26) Bosanquet, C. M. On the Flow of Liquids into Capillary Tubes. *Philos. Mag., Ser. 6* **1923**, *45*, 525.